Nat. Hazards Earth Syst. Sci. Discuss., doi:10.5194/nhess-2016-164, 2016
Manuscript under review for journal Nat. Hazards Earth Syst. Sci.
Published: 21 June 2016

Natural Hazards and Earth System Sciences
Open Access
Discussions

Stand-Alone Tsunami Alarm Equipment

Akio Katsumata[1], Yutaka Hayashi[1], Kazuki Miyaoka[1], Hiroaki Tsushima[1], Toshitaka Baba[2], Patricio A. Catalán[3], Cecilia Zelaya[4], Felipe Riquelme Vasquez[5], Rodrigo Sanchez-Olavarria[6], and Sergio Barrientos[6]

[1]Meteorological Research Institute, Japan Meteorological Agency, Nagamine 1-1, Tsukuba, Ibaraki Prefecture, Japan
[2]Tokushima University, Shinkura-cho 2-24, Tokushima, Tokushima Prefecture, Japan
[3]Federico Santa Maria Technical University, Avenida de - España 1680, Valparaíso, Región de Valparaíso, Chile
[4]Hydrographic and Oceanographic Service, Chilean Navy, Errázuriz Echaurren 254, Playa Ancha, Región Valparaíso, Chile
[5]National Office of Emergency of the Interior Ministry, Calle Beaucheff 1671, Santiago, Región Metropolitana, Chile
[6]University of Chile, Av Libertador Bernardo O'Higgins 1058, Santiago, Región Metropolitana, Chile

Correspondence to: Akio Katsumata (akatsuma@mri-jma.go.jp)

Abstract. One of the quickest means of tsunami evacuation is transfer to higher ground soon after strong and long ground-shaking. Strong ground motion means that the source area of the event is close to the current location, and long ground-shaking or large displacement means that the magnitude is large. We investigated the possibility to apply this to tsunami hazard alarm using single-site ground motion observation. Information from the mass media may not be available sometimes due to power failure. Thus, a device that indicates risk of a tsunami without referring to data elsewhere would be helpful to those should evacuate. Since the sensitivity of a low-cost MEMS accelerometer is sufficient for this purpose, tsunami alarms equipment for home use may be easily realized. Several observation values (e.g., strong-motion duration, peak ground displacement) were investigated as candidates. It was found that a suitable value for a single-site tsunami alarm is long-period peak displacement or the product of strong-motion duration and peak displacement. It was possible to detect an earthquake with a magnitude greater than 7.8 with a 0.8 threat score. Application of this method to recent major earthquakes indicated that such equipment could effectively alert people to the possibility of tsunami.

Key words: Evacuation from tsunami, earthquake magnitude, single-site seismic data processing

1 Introduction

Early-stage tsunami warnings are usually issued by governmental organizations, based on the estimated hypocenter and magnitude. Magnitude, a crucial factor for tsunami forecasting, is estimated based on amplitude of the seismic wave (Katsumata et al. , 2013), rapid estimation of seismic moment (Tsuboi et al. , 1995), or high-frequency energy radiations (Hara , 2007).

If earthquake magnitude can be estimated using ground motion at a single site, residents can be alerted to evacuate due to a possible tsunami without official evacuation messages. Development of low-cost micro electro mechanical systems (MEMS) accelerometers enables equipping an ordinary house with such a single-station tsunami alarm. Some single-site processing methods have been proposed for earthquake early warning. Odaka et al. (2003) developed a method to estimate epicentral distance using single-site seismic data. Magnitude can be estimated based on epicentral distance and amplitude at the station.

Nat. Hazards Earth Syst. Sci. Discuss., doi:10.5194/nhess-2016-164, 2016
Manuscript under review for journal Nat. Hazards Earth Syst. Sci.
Published: 21 June 2016

Natural Hazards and Earth System Sciences
Open Access
Discussions

Allen and Kanamori (2003) used the P-wave predominant period to estimate earthquake magnitude. With tsunami, it is not necessary to focus on the P-wave part of the seismic wave, because it is better to wait for completion of the fault rupture to estimate earthquake magnitude. Moreover the high noise level of a MEMS sensor may result in considerable difference in the estimated value based on P-wave onset. Figure 1 presents examples of epicentral distance estimation from the onset of the P-wave using the method of Odaka et al. (2003), in which sharpness of the onset is used for epicentral-distance estimation. For example, with the 2003 Tokachi-oki earthquake (Fig. 1 (a)), the difference in sharpness of onset estimated with assumption of different noise levels corresponds to 1.6 times the difference in distance. For the 2011 off the Pacific coast of Tohoku earthquake (Fig. 1 (b)), the difference in onset corresponds to 5 times the difference in distance. It is possible to use the whole seismic wave trace for tsunami evacuation purposes. Amplitude is directly related to earthquake magnitude. Strong-motion duration, which is related to earthquake magnitude (Trifunac and Brady , 1975; Dobry et al. , 1978; Izutani and Hirasawa , 1987), is a candidate for single-site magnitude estimation.

Table 1 lists earthquakes that involved ten or more casualties due to tsunamis around the Japanese islands in the past 100 years. This table indicates earthquakes with a magnitude of 8 ($M8$) or greater caused serious disasters. Here we seek to differentiate earthquakes greater than $M8$ from others. We discuss single-station seismic wave processing, focusing on possible application to stand-alone tsunami alarm equipment.

2 Method and Result

Strong ground-shaking generally means that the earthquake fault is close to the observation point. The equipment is considered to have a function of instrumental seismic intensity meter. Here, to limit the area of further judgement, we use instrumental seismic intensity calculated from peak ground velocity following the method of Wald et al. (1999). The higher the threshold intensity, the shorter the fault distance; the lower the intensity, the longer the fault distance. In the present study, we set the seismic intensity to 5.5 (modified Mercalli seismic intensity $\geq$ VI) to limit the area. The seismic intensity of VI is ground-shaking that causes slight fear in people. Si and Midorikawa (1999) presented formulas that relate peak ground velocity on stiff ground to moment magnitude (M_w) and fault distance for various types of earthquakes. We refer to their formula for inter-plate earthquakes. A seismic intensity of 5.5 corresponds to 140 km fault distance for an earthquake of M_w 8.0 based on Si and Midorikawa (1999) and Wald et al. (1999). We use a third-order Butterworth high-pass filter with a cutoff period of 10 s to obtain velocity records from acceleration, following Wald et al. (1999) (Kunugi , 2000).

We investigate the following observation values (V) as possible candidates to distinguish earthquakes with disastrous tsunami potential from smaller ones based on acceleration recorded at a single station.

a Duration above some amplitude level

b Peak ground velocity (PGV)

c Peak ground displacement (PGD)

d Duration $\times$ PGV

Nat. Hazards Earth Syst. Sci. Discuss., doi:10.5194/nhess-2016-164, 2016
Manuscript under review for journal Nat. Hazards Earth Syst. Sci.
Published: 21 June 2016

Natural Hazards and Earth System Sciences
Open Access
Discussions

e Duration × PGD

We use acceleration records obtained with seismic intensity meters installed by the Japan Meteorological Agency . Station locations are indicated in Fig. 2. The epicenters of the events of which seismic records are used in this study are shown also in Fig. 2. Duration here is measured as the period during which instrumental seismic intensity calculated from PGV (Wald et al. , 1999) exceeds 4.5. Whereas this seismic intensity level is arbitrary, corresponding duration level for magnitude discrimination is optimized with the data. We hold the seismic intensity value for 5 s after a peak value is recorded. Velocity and displacement records were obtained by numerical integration from acceleration records. The cutoff period after integration was set at 20 s. Katsumata et al. (2013) proposed a rapid magnitude determination method based on the peak amplitude of various cutoff periods. We selected the period of 20 s, since the magnitude of 20-s cutoff of Katsumata et al. (2013) often agreed well with that of 100-s cutoff. Since we assume the use of a low-cost MEMS accelerometer, the noise level of acceleration is assumed to be 0.2 cm/s^2. Acceleration of 0.2 cm/s^2 is slightly lower than the noticeable tremor level. The 0.2 cm/s^2 of a 20-s period corresponds to 0.6 cm/s in velocity and 2 cm in displacement. We do not use data with less than these amplitudes. The same filter as that of Katsumata et al. (2013) (third-order Bessel filter) is used to obtain displacement records.

We tentatively set two threshold magnitudes (M_{th}), 7.8 and 8.5. Magnitude 7.8 is assumed to indicate an earthquake with the potential of a disastrous tsunami, and the magnitude of 8.5 is assumed to indicate the potential of a huge disaster such as the 2010 Maule earthquake in Chile and the 2011 off the Pacific coast of Tohoku earthquake in Japan. We seek to determine the threshold level of the observation value (V_{th}) that can be used to distinguish large events.

We compare the five values described above based on the threat score as

$$S = \frac{N_{GG}}{N_{GL} + N_{GG} + N_{LG}}, \tag{1}$$

where N_{GG} is the number of data for which $M_w > M_{th}$ and $V > V_{th}$. Likewise N_{GL}, $M_w > M_{th}$ and $V < V_{th}$; N_{LG}, $M_w < M_{th}$ and $V > V_{th}$. The global CMT solutions (Dziewonski et al. , 1981; Ekström et al. , 2012) were referenced for moment magnitude M_w. The result is presented in Fig. 3. The scores are listed in Table 2. A high score is better than a low one. *c* (PGD) and *e* (duration × PGD) indicate high scores. Values related to PGV (*b* and *d*) show lower scores. Whereas the case of *a* (duration) shows a relatively high score, there are some data plots which show small observation values for the event of $M_w > M_{th}$. Two threshold magnitude levels were assumed. However, the difference between optimal observation values is not significant. Figure 4 illustrates the relationship between the score and the observation value. The lobes for $M_{th} = 7.8$ and $M_{th} = 8.5$ overlap, and their peaks are close to one another. Moreover, data is available for only one event with $M_w > 8.5$. It is expected that more reliable results would be obtained for $M_w > 8.5$ if more data were available in that magnitude range. Hereafter, we consider only the case of $M_{th} = 7.8$. This result is obtained using the data in Japan, and applicability to another region is tested in the following section.

Nat. Hazards Earth Syst. Sci. Discuss., doi:10.5194/nhess-2016-164, 2016
Manuscript under review for journal Nat. Hazards Earth Syst. Sci.
Published: 21 June 2016

Natural Hazards and Earth System Sciences
Open Access
Discussions

3 Application to Events

The result is applied to several major earthquakes that occurred around Japan and Chile. The same data used in the previous section are referenced in the trials here for events around Japan. Data archived by the University of Chile are used for events around Chile. Figure 5 represents the results with the observed tsunami heights. The observation value of c (PGD) is applied here. The red dot denotes the station that had observation value and instrumental seismic intensity above the thresholds (Table 2), and were located within 10 km from the shoreline. The orange dot outlined in red denotes a station that was with the both values over the thresholds, but distant from the shoreline. The red open circle denotes a station where instrumental seismic intensity was above the threshold (5.5) but the observation value was below the threshold.

Regarding tsunami height, we referred to runups by Tanioka et al. (2004) for (a), Fritz et al. (2011) for (b), the 2011 Tohoku Earthquake Tsunami Joint Survey Group (2013) for (c), Catalán et al. (2015) for (d), and Aránguiz et al. (2015) for (e). The epicenters are denoted by blue dots, and the source areas are indicated by blue curves. Regarding source areas, we referred to Hatori (2004) for (a), Sladen for (b) (2.5-m slip contour), Yoshida et al. (2011) for (c) (5-m slip contour), wei for (d) (1-m slip contour), and USGS for (e) (2.5-m slip contour). The open contours indicate large slips estimated at the edges of the assumed faults.

In Fig. 5, the observation values of many stations were generally above the threshold in areas of high tsunami. However, such stations did not cover all areas where high tsunamis were observed, and at some stations the observation values were less than the threshold but high tsunamis were observed. For the 2003 Tokachi-oki earthquake (Fig. 5 (a)), the observation values were above the threshold in the areas of high tsunami observation at some stations. However, the number of stations was limited. For the 2010 Maule earthquake (Fig. 5 (b)), the number of the stations was limited; however, the observation values were above the threshold in high-tsunami areas. For the 2011 off the Pacific coast of Tohoku earthquake, the tsunami was high in the northern area due to topographic effects and a large slip near the hypocenter (Mori et al. , 2011). For most high-tsunami areas, the observation values were above the threshold. However, the observation values in the northern part of high tsunami areas were below the threshold, for several possible reasons. For examples, the source area is somewhat far from the coast line in the northern area. Also, the tsunami height of the northern area was affected by the topography of the coastal area. For the 2014 Iquique earthquake, the observation values exceeded the threshold in the area close to the event source. For the 2015 Illapel earthquake, the observation values were above the threshold in the area of highest tsunami.

These examples illustrate that the single station method is effective in promoting evacuation from a large tsunami in many areas, and that it cannot cover the whole area of high-tsunami. Even though this method does not cover a possible disastrous area completely, an alert based on this method may induce caution regarding the possibility of a tsunami after a large earthquake. Moreover, although threshold values were estimated with data obtained in Japan, these examples indicate that this method is applicable to earthquakes around Chile which is located in similar tectonic setting as Japan.

Figure 6 depicts the relationship between magnitude and the number of stations at which the observed value exceeded the threshold. Data with an observation value exceeding the threshold and a magnitude less than M_{th} indicates a false alarm. For PGD, the observation values exceeded the threshold at three stations for two events. Figure 5 (f) presents a map of one of such

Nat. Hazards Earth Syst. Sci. Discuss., doi:10.5194/nhess-2016-164, 2016
Manuscript under review for journal Nat. Hazards Earth Syst. Sci.
Published: 21 June 2016

Natural Hazards and Earth System Sciences
Open Access
Discussions

events. The moment magnitude of the event of Fig. 5 (f) was 6.7. Large amplitudes were observed at stations very close to the source area in this case. Duration × PGD indicates the fewest false alarm in Fig. 6. However, duration × PGD results in more misses than PGD.

We built prototype tsunami alarm equipment using a MEMS sensor and a small computer, and tentatively observed ground motion with it. Records were obtained for the 2015 Illapel earthquake at the site of 33.03° S, 77.64° W. Figure 7 indicates the observed acceleration, velocity for calculating instrumental seismic intensity, instrumental seismic intensity, and displacement to obtain the PGD value. ONEMI reported seismic intensity at this region (Valparaíso) as VI, which is close to the value obtained with the prototype equipment (V). Since the observation point was far from the source area, the seismic intensity did not reach the threshold. However, the result indicates that a MEMS sensor could work for this purpose.

4 Conclusions

We proposed a method to differentiate earthquakes with disastrous tsunami potential from others using ground motion at a single station. With this method, the area is limited by the condition of high seismic intensity, and the earthquake magnitude is differentiated using peak ground displacement. The product of strong-motion duration and peak ground displacement showed similar result of peak ground displacement solely. It is possible to develop small equipment for this purpose using a low-cost MEMS sensor.

Application of this method to recent major earthquakes indicated that this method is partially effective in informing people of the possibility of a disastrous tsunami. We do not intend that this method would provide a perfect tsunami alarm system; rather, we expect this method to work as a complement to the alarm of governmental organizations.

Data availability

Acceleration records obtained by the seismic intensity meters of the Japan Meteorological Agency are available at http://www.data.jma.go.jp/svd/eqev/data/kyoshin/jishin/index.html. Acceleration records obtained by the University of Chile are available at http://evtdb.csn.uchile.cl. The data of hypocenters of the unified seismic catalog in Japan are available at http://www.data.jma.go.jp/svd/eqev/data/bulletin/hypo.html.

Acknowledgements. This study used strong motion data obtained by the Japan Meteorological Agency and the University of Chile. We referred to hypocenter locations estimated using the seismic data of the National Research Institute for Earth Science and Disaster Prevention, Hokkaido University, Hirosaki University, Tohoku University, the University of Tokyo, Nagoya University, Kyoto University, Kochi University, Kyushu University, Kagoshima University, the National Institute of Advanced Industrial Science and Technology, the Tokyo metropolitan government, the Shizuoka Prefectural government, the Kanagawa Prefectural government, the City of Yokohama, the Japan Marine Science and Technology Center, and the Japan Meteorological Agency. This study was partly supported by the SATREPS research project of "Enhancement of technology to develop tsunami-resilient community".

References

Allen, R. M., and Kanamori, H.: The potential for earthquake early warning in southern California, Science, 300, 786-789, 2003.

Aránguiz, R., González, G., González, J., Catalán, P. A., Cienfuegos, R., Yagi, Y., Okuwaki, R., Urra, L., Contreras, K., Rio, I. D., and Rojas, C.: The 16 September 2015 Chile Tsunami from the post-tsunami survey and numerical modeling perspectives, Pure Appl. Geophys., 173, 333-348, doi:10.1007/s00024-015-1225-4, 2015.

Catalán, P. A., Aránguiz,R., González, G., Tomita, T., Cienfuegos, R., González, J., Shrivastava, M. N., Kumagai, K., Mokrani, C., Cortés, P., and Gubler, A., The 1 April 2014 Pisagua tsunami: Observations and modeling, Geophys. Res. Lett., 42, 2918-2925, doi:10.1002/2015GL063333, 2015.

Dobry, R., Idriss, I. M., and Ng, E.: Duration characteristics of horizontal components of strong-motion earthquake records, B. Seismol. Soc. Am., 68, 1487-1520, 1978.

Dziewonski, A. M., Chou T.-A., and Woodhouse, J. H.: Determination of earthquake source parameters from waveform data for studies of global and regional seismicity, J. Geophys. Res., 86, 2825-2852, doi:10.1029/JB086iB04p02825, 1981.

Ekström, G., Nettles, M., and Dziewonski, A. M.: The global CMT project 2004-2010: Centroid-moment tensors for 13,017 earthquakes, Phys. Earth Planet. In., 200-201, 1-9, doi:10.1016/j.pepi.2012.04.002, 2012.

Fritz, H. M., Petroff, C. M., Catalán, P. A., Cienfuegos, R., Winckler, P., Kalligeris, N., Weiss, R., Barrientos, S. E., Meneses, G., Valderas-Bermejo, C., Ebeling, C., Papadopoulos, A., Contreras, M., Almar, R., Dominguez, J. C., and Synolakis, C. E.: Field survey of the 27 February 2010 Chile tsunami, Pure Appl. Geophys., 168, 1989-2010, doi:10.1007/s00024-011-0283-5, 2011.

Hara, T.: Magnitude determination using duration of high frequency energy radiation and displacement amplitude: application to tsunami earthquakes, Earth Planets Space, 59, 561-565, 2007.

Hatori, T.: Size and source area of 2003 Tokachi-oki earthquake, Research Reports of Tsunami Engineering, Disaster Control Research Center, Tohoku University, 21, 93-98, 2004. (in Japanese)

Izutani, Y., and Hirasawa, T.: Use of strong motion duration for rapid evaluation of fault parameters, J. Phys. Earth, 35, 171-190, 1987.

Japan Meteorological Agency, Strong motion data: http://www.data.jma.go.jp/svd/eqev/data/kyoshin/jishin/index.html, last access: 12 Feb., 2015.

Katsumata, A., Ueno, H., Aoki, S., Yoshida, Y., and Barrientos, S.: Rapid magnitude determination from peak amplitudes at local stations, Earth Planets Space, 65, 843-853, doi:10.5047/eps.2013.03.006, 2013.

Kunugi, T.: Relationship between Japan Meteorological Agency instrumental intensity and instrumental modified Mercalli intensity obtained from K-NET strong-motion data, , J. Seismol. Soc. Jpn, 53, 89-93, 2000. (in Japanese with English abstract)

Mori, N., Takahashi, T., Yasuda, T., and Yanagisawa, H.: Survey of 2011 Tohoku earthquake tsunami inundation and run-up, Geophys. Res. Lett., 38, L00G14, doi:10.1029/2011GL049210, 2011.

Moroi, T. and Takemura, M.: Mortality estimation by causes of death due to the 1923 Kanto Earthquake, J. Japan Assoc. Earth. Eng., 4, 4, 21-35, 2004. (in Japanese)

National Police Agency, Damages by the 2011 off the Pacific coast of Tohoku earthquake and measures implemented by th police: https://www.npa.go.jp/archive/keibi/biki/higaijokyo.pdf, last access: 17 Sept., 2015.

Odaka, T., Ashiya, K., Tsukada, S., Sato, S., Ohtake, K., and Nozaka, D.: A new method of quickly estimating epicentral distance and magnitude from a single seismic record, B. Seismol. Soc. Am., 93, 526-532, 2003.

Nat. Hazards Earth Syst. Sci. Discuss., doi:10.5194/nhess-2016-164, 2016
Manuscript under review for journal Nat. Hazards Earth Syst. Sci.
Published: 21 June 2016

Natural Hazards and Earth System Sciences
Open Access
Discussions

ONEMI, Earthquake of greater intensity between the regions of Atacama and La Araucania: http://www.onemi.cl/informate/sismo-de-mayor-intensidad-en-las-regiones-de-metropolitana-y-maule/, last access: 30 March, 2016.

Si, H. and Midorikawa, S.: New attenuation relationships for peak ground acceleration and velocity considering effects of fault type and site condition, Journal of Struct. Construct. Eng., AIJ, ,523, 63-70, 1999. (in Japanese)

Sladen A.: Preliminary Result 02/27/2010 (M_w 8.8) Chile, Source Models of Large Earthquakes: http://www.tectonics.caltech.edu/slip_history/2010_chile/index.html, last access: 9 Dec. 9, 2015.

Tanioka, Y., Nishimura, Y., Hirakawa, K., Imamura, F., Abe, I., Abe, Y., Shindou, K., Matsutomi, H., Takahashi, T., Imai, K., Harada, K., Namegawa, Y., Hasegawa, Y., Hayashi, Y., Nanayama, F., Kamataki, T., Kawata, Y., Fukasawa, Y., Koshimura, S., Hada, Y., Azumai, Y., Hirata, K., Kamikawa, A., Yoshikawa, A., Shiga, T., Kobayashi, M., and Masaka, S.: Tsunami run-up heights of the 2003 Tokachi-oki earthquake, Earth Planets Space, 56, 359-365, 2004.

The 2011 Tohoku Earthquake Tsunami Joint Survey Group, The 2011 off the Pacific coast of Tohoku earthquake tsunami information: http://www.coastal.jp/ttjt, last access: 6 Dec., 2015.

Trifunac, M. D. and Brady, A. G.: A study on the duration of strong earthquake ground motion, B. Seismol. Soc. Am., 65, 581-626, 1975.

Tsuboi, S., Abe, K., Takano, K., and Yamanaka, Y.: Rapid determination of M_w from broadband P waveforms, B. Seismol. Soc. Am., 85, 606-613, 1995.

Usami, T.: Materials for comprehensive list of destructive earthquakes in Japan [416]-2001 [Latest Edition], 605 pp., University of Tokyo Press, Tokyo, 2003. (in Japanese)

USGS, Preliminary finite fault results for the Sep 16, 2015 M_w 8.3 46 km W of Illapel, Chile Earthquake (Version 1): http://earthquake.usgs.gov/archive/product/finite-fault/us20003k7a/us/1442454346406/web/20003k7a.fsp, last access: 15 Feb. 15, 2016.

Wald, D. J., Quitoriano, V., Heaton, T. H., and Kanamori, H.: Relationships between peak ground acceleration, peak ground velocity, and modified Mercalli intensity in California, Earthq. Spectra: August 1999, 15, 557-564, 1999.

Wei, S.: Apr./01/2014 (Mw 8.1), Iquique, Chile, Source Models of Large Earthquakes: http://www.tectonics.caltech.edu/slip_history/2014_chile/index.html, last access: 15 Feb. 15, 2016.

Yoshida, Y., Ueno, H., Muto, D., and Aoki, S.: Source process of the 2011 off the Pacific coast of Tohoku Earthquake with the combination of teleseismic and strong motion data, Earth Planets Space, 63, 565-569, doi:10.5047/eps.2011.05.011, 2011.

Nat. Hazards Earth Syst. Sci. Discuss., doi:10.5194/nhess-2016-164, 2016
Manuscript under review for journal Nat. Hazards Earth Syst. Sci.
Published: 21 June 2016

Natural Hazards and Earth System Sciences
Open Access
Discussions

Table 1. Major disastrous earthquakes and casualties due to their tsunami around the Japanese Islands in the past 100 years.

Origin time (JST)	Epicenter	Casualties including the missing	M
1 September, 1923 at 11:58	139.14° E, 35.33° N	325(105,385)*1	7.9
3 March, 1933 at 02:30	145.12° E, 39.13° N	3,064*2	8.1
2 August, 1940 at 00:08	139.81° E, 42.36° N	10*2	7.5
7 December, 1944 at 13:35	136.18° E, 33.57° N	(1,251)*2	7.9
21 December, 1946 at 04:19	135.85° E, 32.94° N	(1,443)*2	8.0
4 March, 1952 at 10:23	144.15° E, 41.71° N	(33)*2	8.2
26 May, 1983 at 11:59	139.07° E, 40.36° N	100(104)*2	7.7
12 July, 1993 at 22:17	139.18° E, 42.78° N	(230)*2	7.8
11 March, 2011 at 14:46	142.85° E, 38.10° N	18,465*3	9.0

Numbers in parentheses indicate total casualties including those due to causes other than tsunami: *1, Moroi and Takemura (2004); *2, Usami (2003); *3, National Police Agency (2015). The unified seismic catalog of Japan was referenced to for the epicenter and magnitude.

Nat. Hazards Earth Syst. Sci. Discuss., doi:10.5194/nhess-2016-164, 2016
Manuscript under review for journal Nat. Hazards Earth Syst. Sci.
Published: 21 June 2016

Natural Hazards and Earth System Sciences
Open Access
Discussions

Table 2. Peak threat scores for various observation values.

M_{th}	S_a	S_b	S_c	S_d	S_e
7.8	0.73(1.80)	0.47(1.13)	0.80(0.95)	0.66(2.90)	0.79(2.90)
8.5	0.75(1.91)	0.35(1.31)	0.62(1.10)	0.59(3.05)	0.75(3.13)

S_a, threat score for strong motion duration; S_b, for PGV; S_c, for PGD; S_d, for duration $\times$ PGV; S_e, for duration $\times$ PGD. The values in parentheses are the logarithmic ($\log_{10}$) observation values that indicated peak threat scores. The units of the observation values are logarithm of s, cm/s, cm, s·cm/s, and s·cm.

Nat. Hazards Earth Syst. Sci. Discuss., doi:10.5194/nhess-2016-164, 2016
Manuscript under review for journal Nat. Hazards Earth Syst. Sci.
Published: 21 June 2016

Natural Hazards and Earth System Sciences
Open Access
Discussions

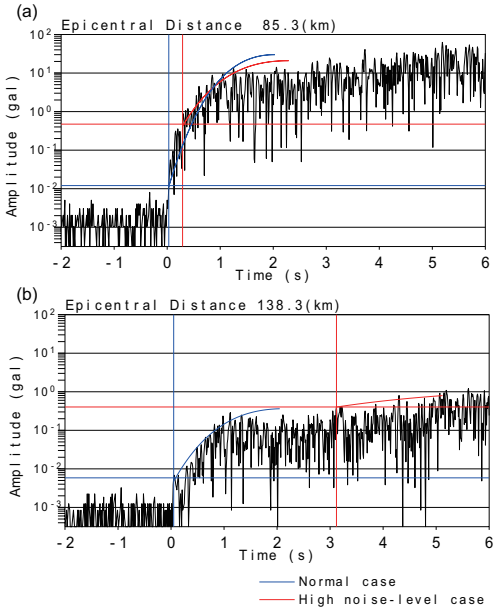

Figure 1. Examples of epicentral distance estimation using the method of Odaka et al. (2003). (a) Record of the 2003 Tokachi-oki earthquake on 26 Sept., 2003; (b) record of the 2011 off the Pacific coast of Tohoku earthquake on 11 March, 2011. Two levels of noise were assumed. Blue lines: the curve of $Bt\exp(-At)$ (refer to Okada et al., 2003) was fitted for the part where amplitude exceeded double the noise level. Red lines: the curve was fitted for the part where the amplitude exceeded 0.4 gal, which was assumed to be twice the noise level of a MEMS sensor.

Nat. Hazards Earth Syst. Sci. Discuss., doi:10.5194/nhess-2016-164, 2016
Manuscript under review for journal Nat. Hazards Earth Syst. Sci.
Published: 21 June 2016

Natural Hazards and Earth System Sciences
Open Access
Discussions

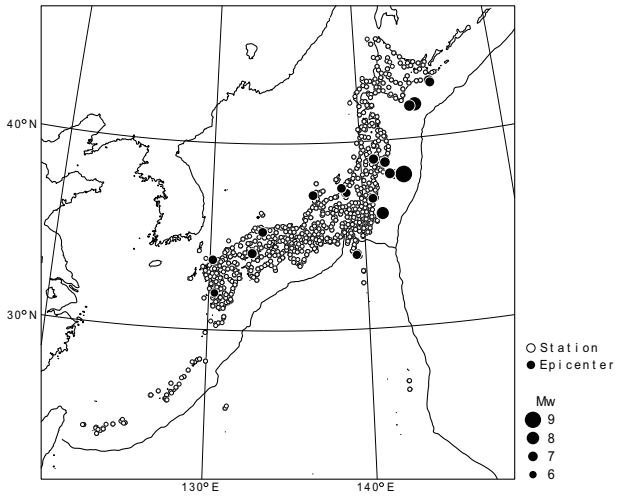

Figure 2. Station and epicenter map. Stations of seismic intensity meters (open circles), and epicenters of the events (solid circles) for which seismic records were used in this study are denoted.

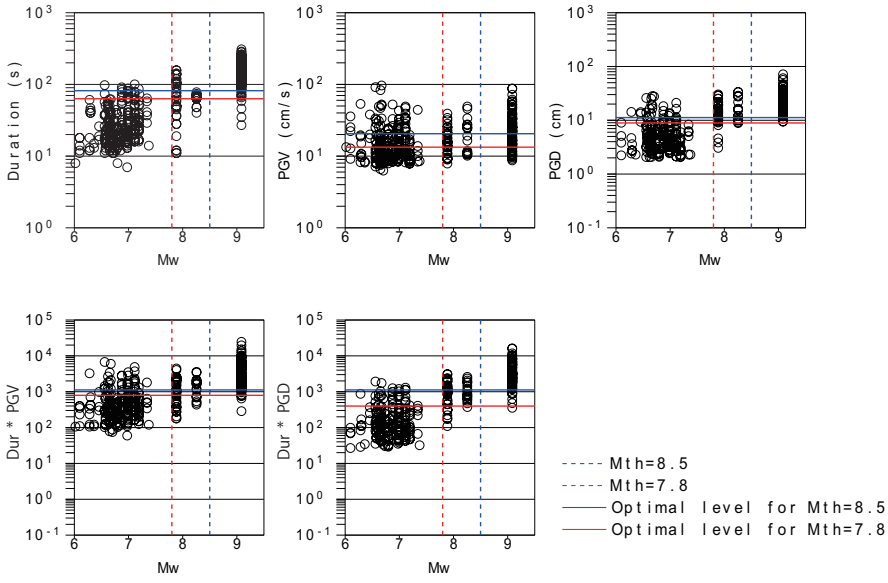

Figure 3. Relationship between observation values and M_w. The observation value is strong motion duration (Dur), peak ground velocity (PGV), peak ground displacement (PGD), product of duration and PGV, or product of duration and PGD.

Nat. Hazards Earth Syst. Sci. Discuss., doi:10.5194/nhess-2016-164, 2016
Manuscript under review for journal Nat. Hazards Earth Syst. Sci.
Published: 21 June 2016

Natural Hazards and Earth System Sciences
Open Access
Discussions

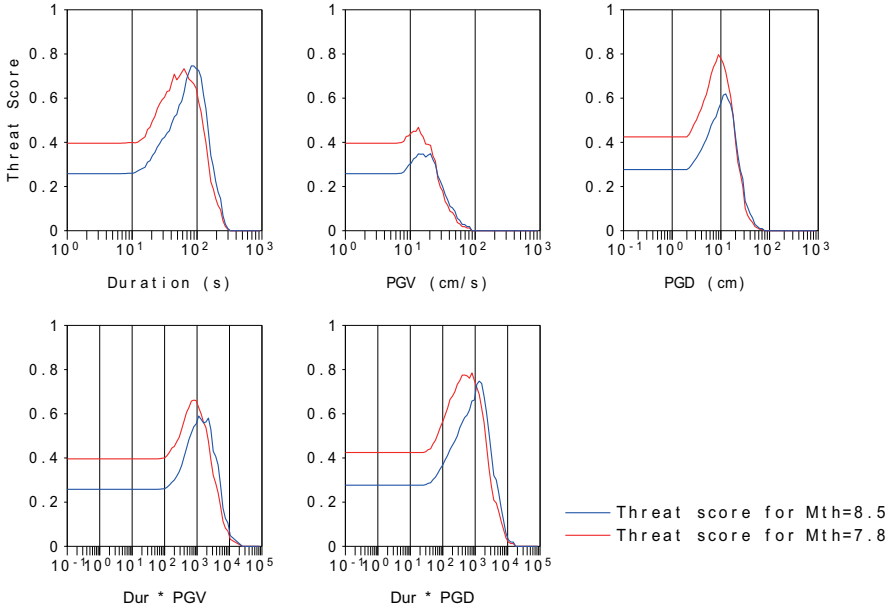

Figure 4. Relationship between threat score and observed values.

Nat. Hazards Earth Syst. Sci. Discuss., doi:10.5194/nhess-2016-164, 2016
Manuscript under review for journal Nat. Hazards Earth Syst. Sci.
Published: 21 June 2016

Natural Hazards and Earth System Sciences
Open Access
Discussions

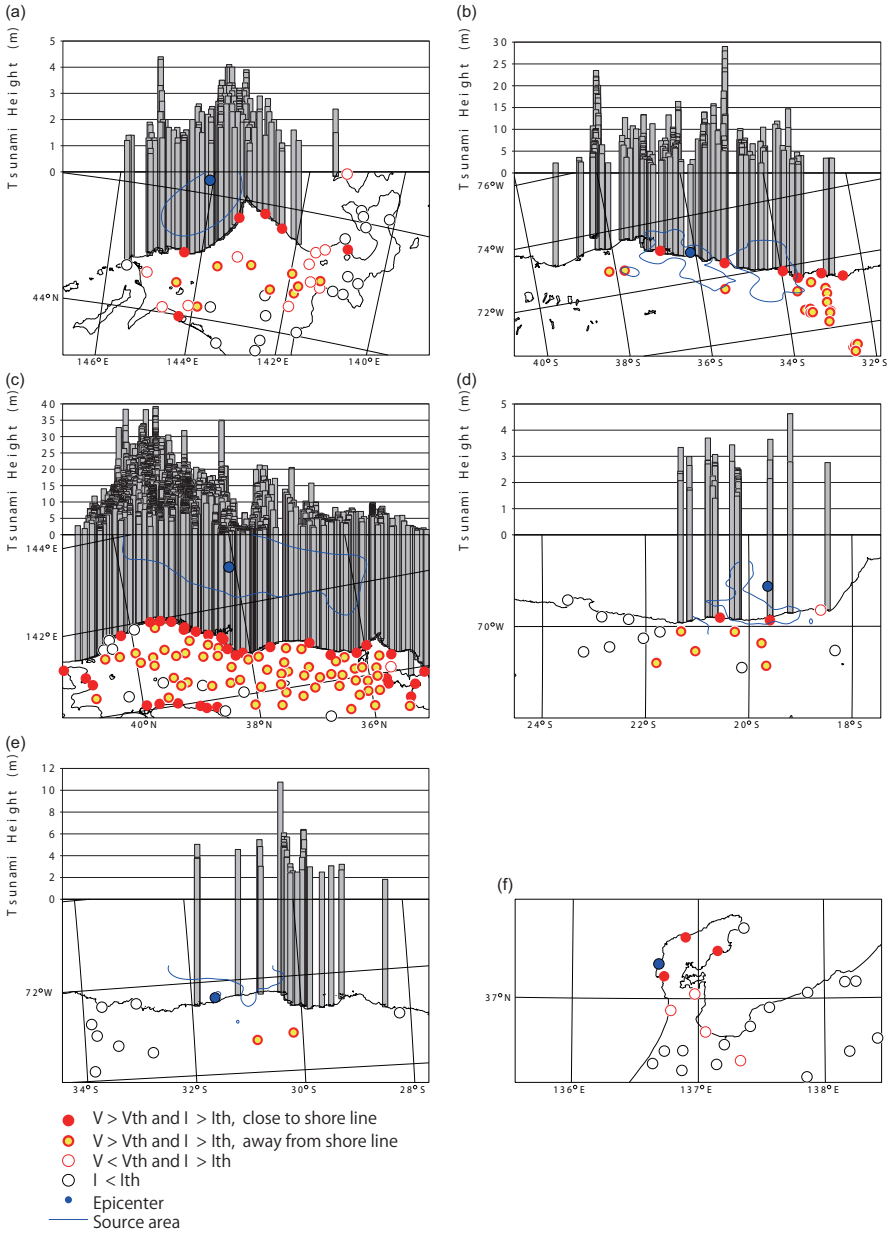

Figure 5. Map plot of the observation values for major earthquakes. (a) the 2003 Tokachi-oki earthquake (M_w 8.3), (b) the 2010 Maule Earthquake (M_w 8.8), (c) the 2011 off the Pacific coast of Tohoku earthquake (M_w 9.1), (d) the 2014 Iquique earthquake (M_w 8.1), (e) the 2015 Illapel earthquake (M_w 8.3), (f) the Noto Hanto earthquake in 2007 (M_w 6.6). Color is classified according to observation value (V) and instrumental seismic intensity (I) compared with threshold values (V_{th}, I_{th}). The observed tsunami runup heights are also indicated.

Nat. Hazards Earth Syst. Sci. Discuss., doi:10.5194/nhess-2016-164, 2016
Manuscript under review for journal Nat. Hazards Earth Syst. Sci.
Published: 21 June 2016

Natural Hazards and Earth System Sciences
Open Access
Discussions

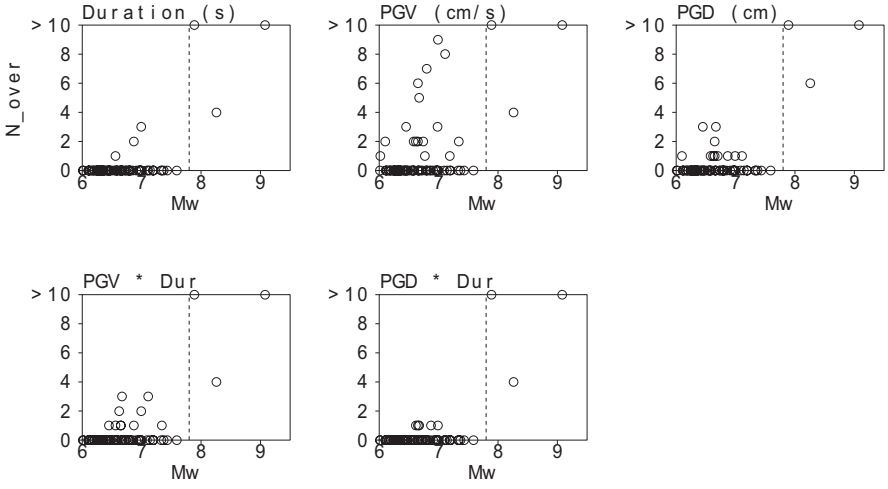

Figure 6. Relationship between magnitude and number of stations where the observed values exceeded the threshold (Table 2). The vertical broken line indicates magnitude of 7.8, which was set as the threshold magnitude.

Nat. Hazards Earth Syst. Sci. Discuss., doi:10.5194/nhess-2016-164, 2016
Manuscript under review for journal Nat. Hazards Earth Syst. Sci.
Published: 21 June 2016

Natural Hazards and Earth System Sciences
Open Access
Discussions

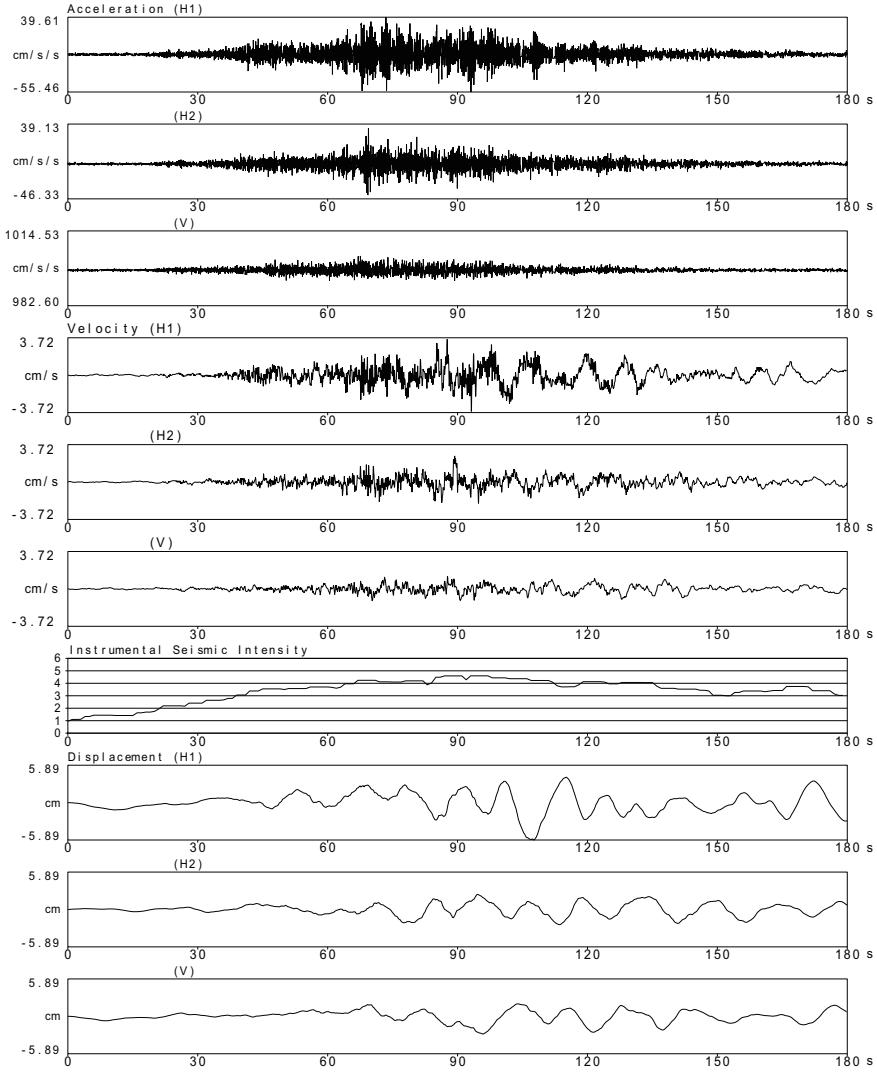

Figure 7. Seismic waves and instrumental seismic intensity obtained using prototype tsunami-alarm equipment. Original acceleration records, velocity records for instrumental seismic intensity, instrumetal seismic intensity, and displacement records are shown.